TYPE OF NON-LINEARITY OF SHALLOW SPHERICAL SHELLS USING NON-LINEAR NORMAL MODES.

Cyril Touzé
ENSTA-Unité de Mécanique (UME)
Chemin de la Hunière
91761 Palaiseau Cedex, France
Cyril.Touze@ensta.fr

Olivier Thomas
CNAM-Structural Mechanics
and coupled systems Laboratory
2 rue Conté, 75003 Paris, France
olivier.thomas@cnam.fr

Abstract

Large amplitude vibrations of free-edge shallow spherical shells, including geometrical non-linearities, are investigated. The analog for thin shallow shells of Von Kármán's theory for large deflection of plates is used. The analysis is focused on the type of non-linearity (hardening/softening behaviour) displayed by the shell, as a function of its geometry (radius of curvature R, thickness h and outer diameter $2a$). For an accurate prediction, non-linear normal modes (NNMs) are used, as a single NNM enables prediction of the correct type of non-linearity, contrary to the associated linear normal modes. The transition from hardening (flat plate) to softening behaviour (occuring for large curvature), is studied. The importance of 2:1 internal resonance is underlined.

Key words

spherical shells, hardening/softening behaviour.

1 Introduction

Non-linear (large-amplitude) vibration of continuous structures such as arches, suspended cables or shells, is a problem of widespread relevance from the engineering as well as from the theoretical viewpoint. Despite numerous studies on these subjects, some important features still remain partially or completely unsolved, due to the intrinsic non-linear nature of the problem. For such structures with an initial curvature in the middle surface, the presence of both quadratic and cubic non-linearities renders the prediction of the type of non-linearity (i.e. the hardening or softening behaviour displayed by each mode of the structure) a difficult problem. For example, the type of non-linearity for circular cylindrical shells has been the subject of a number of studies and controversial discussions since the sixties, see [Amabili and Païdoussis, 2003] for a recent review on the subject.

The main difficulty relies in the truncation one has to use for analyzing the PDE of motion. It has been shown that too severe truncations (using for example a single linear mode) may predict an incorrect type of non-linearity, due to specific interactions, neglected in the approximated solution.

One method to overcome these errors consists in keeping numerous basis functions and perform intensive numerical computations in order to derive the correct type of non-linearity. This has been successively achieved in [Pellicano, Amabili and Païdoussis, 2002] for circular cylindrical shells.

An alternative consists in using reduced-order models that are able to predict the correct type of non-linearity, while still keeping a single oscillator-equation. Non-linear normal modes (NNMs), defined as invariant manifolds in phase space and computed by real normal form theory, offers a clean framework to perform these kind of analysis, as it has been shown in [Touzé, Thomas and Chaigne, 2004]. It is the aim of the present contribution to use this methodology in order to predict the correct type of non-linearity displayed by shallow spherical shells, as a function of its geometry (radius of curvature R, thickness h and outer diameter $2a$).

A model for the geometrically non-linear vibrations of free-edge shallow spherical shells, based on the analog of Von Karman's theory for large deflection of plates, is briefly recalled [Thomas, Touzé and Chaigne, 2005]. NNMs are then used to derive the analytical expression of the term governing the type of non-linearity, for each mode of the shell: axisymmetric as well as asymmetric. This term is then numerically computed as a function of the aspect ratio of the shell. Flat plates (obtained as R tends to infinity) are known to display a hardening behaviour, whereas shells generally behaves in a softening way.

The transition between these two types of non-linear behaviour is explicitely studied, and the specific role of 2:1 internal resonance in this process is clarified.

2 Non-linear model of the shell

2.1 Local equations

A spherical shell of thickness h, radius of curvature R and outer diameter $2a$, made of a homogeneous isotropic material of density ρ, Poisson ratio ν and Young's modulus E, is considered (see fig 1). Large transverse deflections and moderate rotations are taken into account, so that the model is a generalization of Von Kármán's theory for large deflection of plates. Two supplementary geometrical assumptions are considered: the shell is *thin* (so that $h/a \ll 1$ and $h/R \ll 1$), and *shallow* (so that $a/R \ll 1$). As

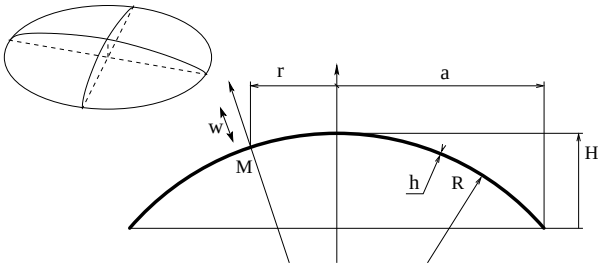

Figure 1. Geometry of the shell: three-dimensional sketch and cross section.

this study is concerned with the type of non-linearity, which is dictated by the conservative problem, damping and external forces are not taken into account. Dimensionless variables are here directly considered, so that the equations of motion are given in terms of the dimensionless transverse displacement w along the normal to the mid-surface and the dimensionless Airy stress function F, for all time t:

$$\Delta\Delta w + \varepsilon_q \, \Delta F + \ddot{w} = \varepsilon_c \, L(w, F), \qquad \text{(1a)}$$

$$\Delta\Delta F - \sqrt{\kappa}\Delta w = -\frac{1}{2} L(w, w), \qquad \text{(1b)}$$

where $\ddot{w}$ is the second partial derivative of w with respect to time, Δ is the laplacian and L is a bilinear quadratic operator. With the assumption of a shallow shell fulfilled, the spatial operators are written in polar coordinates, see [Thomas, Touzé and Chaigne, 2005].

The aspect ratio κ of the shell has been introduced:

$$\kappa = \frac{a^4}{R^2 \, h^2}, \qquad (2)$$

as well as the two parameters ε_q and ε_c, governing the balance between the quadratic and the cubic terms. They read:

$$\varepsilon_q = 12(1-\nu^2)\frac{a^2}{Rh} = 12(1-\nu^2)\sqrt{\kappa}, \qquad \text{(3a)}$$

$$\varepsilon_c = 12(1-\nu^2). \qquad \text{(3b)}$$

Free-edge boundary conditions are considered:

$$F \text{ and } w \text{ are bounded at } r = 0, \qquad \text{(4a)}$$

$$F_{,r} + F_{,\theta\theta} = 0\,, \quad F_{,r\theta} + F_{,\theta} = 0\,, \quad \text{at } r = 1, \qquad \text{(4b)}$$

$$w_{,rr} + \nu w_{,r} + \nu w_{,\theta\theta} = 0\,, \quad \text{at } r = 1, \qquad \text{(4c)}$$

$$w_{,rrr} + w_{,rr} - w_{,r} + (2-\nu) w_{,r\theta\theta} - (3-\nu) w_{,\theta\theta} = 0\,, \quad \text{at } r = 1. \qquad \text{(4d)}$$

2.2 Linear analysis

Analytical expressions of the eigenmodes $\Phi_{k,n}(r,\theta)$, as well as their associated eigenfrequencies $\omega_{k,n}$, are derived from the linear part of Eq. (1). The main results arising from this linear analysis, provided in [Thomas, Touzé and Chaigne, 2005], are here briefly recalled:

- Eigensolutions are described by a set of two real numbers (k,n), where k refers to the number of nodal diameters of the mode shape, and n to the number of nodal circles. Asymmetric modes (such that $k \geq 1$) are degenerated since the associated eigenvalues have multiplicity two. Thus two independent modes are taken into account for each asymmetric eigenfrequency (*preferential configurations*).
- Purely asymmetric modes (with no nodal circles) are distinguished since their eigenfrequencies show a very slight dependence on curvature, see Fig. 2.
- On the other hand, axisymmetric modes (with no nodal diameter) as well as mixed modes (asymmetric with at least one nodal circle) show a huge eigenfrequency dependence on curvature.

2.3 Modal expansion

The complete non-linear equations of motion (1) are projected onto the natural basis of the transverse eigenmodes. The displacement is thus written as:

$$w(r,\theta,t) = \sum_{p=1}^{+\infty} X_p(t) \, \Phi_p(r,\theta), \qquad (5)$$

where the subscript p refers to a specific mode of the shell, defined by a couple $(k,\, n)$ and, if $k \neq 0$, a binary variable which indicates the preferential configuration considered. The modal displacements X_p

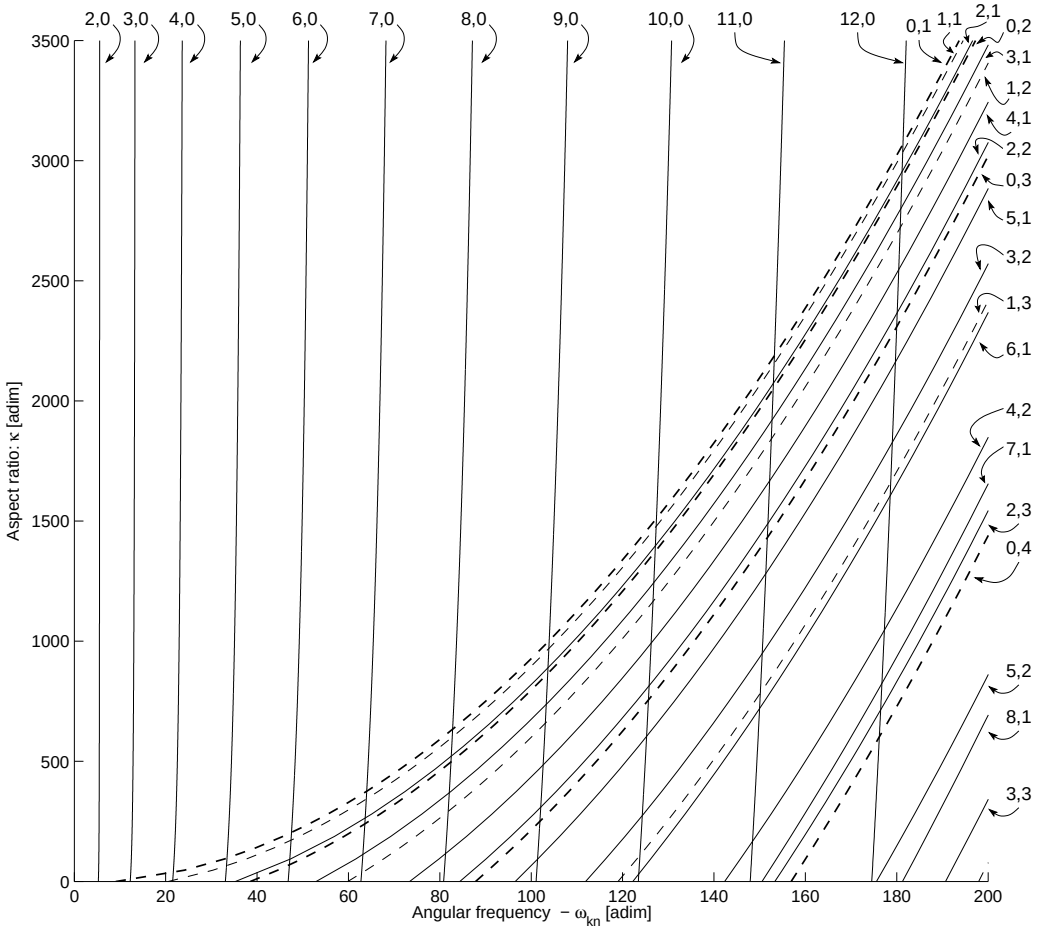

Figure 2. Dimensionless natural frequencies ω_{kn} of the shell as a function of the aspect ratio κ, for ν=0.33.

are the unknowns, and their dynamics is governed by: $\forall\, p \geq 1$:

$$\ddot{X}_p + \omega_p^2 X_p + \varepsilon_q \sum_{i=1}^{+\infty}\sum_{j=1}^{+\infty} \beta_{ij}^p X_i X_j + \varepsilon_c \sum_{i=1}^{+\infty}\sum_{j=1}^{+\infty}\sum_{k=1}^{+\infty} \Gamma_{ijk}^p X_i X_j X_k = 0. \quad (6)$$

The non-linear physical coefficients $\{\beta_{ij}^p\,,\ \Gamma_{ijk}^p\}$ are computed from integrals involving the mode shapes of the connected eigenmodes; their analytical expression can be found in [Thomas, Touzé and Chaigne, 2005]. As a result of the rotational symmetry of the structure, a number of them vanishes, which renders some modal interaction impossible, even though the relationship on the eigenfrequencies is fulfilled.

3 Type of non-linearity

3.1 Analytical derivation

Computing the correct type of non-linearity for structures displaying quadratic and cubic non-linearities has been a controversial subject in the past mainly because erroneous results were derived on the basis of too severe truncations. Keeping only the p^{th} oscillator-equation from Eq. (6) by letting $X_j = 0\ \forall j \neq p$ may produce incorrect prediction, as shown for example in [Nayfeh, Nayfeh and Mook, 1992]. On the mathematical viewpoint, it can be said that the type of non-linearity is governed by the cubic non-linear terms, which is of the second-order (in amplitude) in an asymptotic development, as compared to the first-order perturbation caused by the quadratic terms. Thus an acceptable methodology needs to process the quadratic terms in a correct fashion, *i.e.* the effect of all the quadratic terms on a single oscillator have to be taken into account.

Non-linear normal modes (NNMs), defined as invariant manifolds in phase space, have been defined with the objective of embedding the main dynamical features of a N-dof system into a single non-linear equation, hence providing accurate reduced-order models for non-linear analysis/synthesis. Proper truncations can be realized, as the motion is described in an invariant-based span of the phase space, and thus non-resonant coupling terms between oscillators

have been cancelled. Keeping a single non-linear mode predicts the correct type of non-linearity, as it has been demonstrated and numerically verified on continuous beam-like systems [Touzé, Thomas and Chaigne, 2004; Touzé, Thomas and Huberdeau, 2004].

A first-order perturbative development of the amplitude-frequency relationship on the p^{th} NNM gives:

$$\omega_{NL} = \omega_p(1 + T_p a^2), \tag{7}$$

where a is the amplitude of the response of the p^{th} NNM and T_p the coefficient governing the type of non-linearity. If $T_p > 0$, then hardening behaviour occurs, whereas $T_p < 0$ implies softening behaviour. The analytical expression of T_p reads:

$$T_p = \frac{1}{8\omega_p^2}\left[3(A^p_{ppp} + \varepsilon_c \Gamma^p_{ppp}) + \omega_p^2 B^p_{ppp}\right], \tag{8}$$

where:

$$A^p_{ppp} = \varepsilon_q^2 \sum_{l=1}^{+\infty} \frac{2\omega_p^2 - \omega_l^2}{D_{pl}} (\beta^p_{pl} + \beta^p_{lp})\beta^l_{pp}\,, \tag{9}$$

$$B^p_{ppp} = \varepsilon_q^2 \sum_{l=1}^{+\infty} \frac{2}{D_{pl}} (\beta^p_{pl} + \beta^p_{lp})\beta^l_{pp}\,, \tag{10}$$

$$D_{pl} = \omega_l^2(\omega_l - 2\omega_p)(\omega_l + 2\omega_p). \tag{11}$$

One can see that the influence of all the linear modes are taken into account to compute the type of non-linearity of a single mode. The usual cubic coefficient of the p^{th} oscillator (Γ^p_{ppp}) is balanced by the infinite sumations standing in the formula defining A^p_{ppp} and B^p_{ppp}. Moreover, inspection of these sumations and comparison with the rules for a non-vanishing quadratic coefficient allows one to select the important modes which are able to act on the sign of T_p.

As shown in [Thomas, Touzé and Chaigne, 2005], the conditions for the $\{\beta^p_{ij}\}_{p,i,j\geq 1}$ to be non-zero are expressed in terms of the number of nodal diameters k_l and k_p of the l and p modes. They read:

(i) $\beta^l_{pp} \neq 0$ if $k_l \in \{2k_p, 0\}$.
(ii) $\beta^p_{pl} \neq 0$ or $\beta^p_{lp} \neq 0$ if $k_p \in \{k_l + k_p,\ |k_l - k_p|\}$.

These rules show that two classes of modes have to be retained when studying the type of non-linearity of the p^{th} mode: axisymmetric ($k_l = 0$) as well as asymmetric modes having twice the number of nodal diameters ($k_l = 2k_p$). No other mode has an influence on the type of non-linearity.

In the remainder of the study, N will refer to the number of modes retained in this specific subset composed of the pertinent ones with respect to the type of non-linearity. When $N = 1$, the formula (8) reduces to that obtained when keeping a single-mode in the truncation. Modal truncation will be studied by increasing N until convergence.

3.2 2:1 Internal resonance

An interesting point arising from the analytical formula of T_p, and especially Eq. (11), is that there is only one kind of internal resonance, namely 2:1 resonance, which have an influence on the type of non-linearity. When studying the p^{th} mode, only the l^{th} modes, whose eigenfrequencies are such that $\omega_l = 2\omega_p$, are able to significantly change the value of T_p. Other second-order internal resonances are not able to produce a small denominator and to change the value of T_p.

In case of 2:1 internal resonance, a first-order perturbative study shows that *only coupled solutions are possible*. Thus the type of non-linearity, which is a notion associated to the backbone curve of a single oscillator, does not have anymore meaning. In the following sections, concerned with the numerical results, it will be seen that the value of T_p diverges to infinity when encountering a 2:1 internal resonance. On a physical viewpoint, these values does not have sense, and the calculation presented here is not valid in a small interval around the resonance value.

4 Numerical results

In this section, numerical computations of T_p as a function of the aspect ratio κ of the shell, are presented. Purely asymmetric modes are first considered, then axisymmetric and mixed modes. The main time-consuming task in the numerical effort, when N becomes large, is the computation of all the quadratic coefficients $\{\beta^k_{ij}\}_{k,i,j=1\ldots N}$, needed to construct the summations. In order to save time, advantage has been taken of their slight dependence with respect to the aspect ratio κ: quadratic coefficients are kept constant on small κ-intervals, instead of computing them for each value of the aspect ratio.

4.1 Purely asymmetric modes

The results for two purely asymmetric modes, namely (2,0) and (5,0), will be here shown, and general conclusion will be derived from these two examples. The Poisson ratio is $\nu = 0.33$ for all the presented results. For any purely asymmetric mode $(k, 0)$, the truncation rules provided in the precedent section show that two families of modes have to be retained : axisymmetric ones, and purely asymmetric of the form $(2k, 0)$.

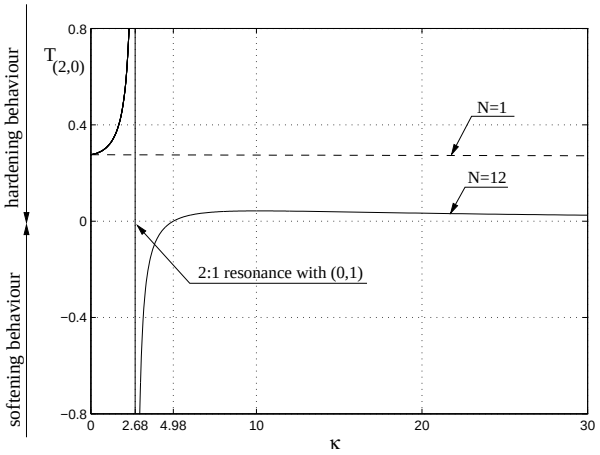

Figure 3. Type of non-linearity for the fundamental (2,0) mode with respect to κ.

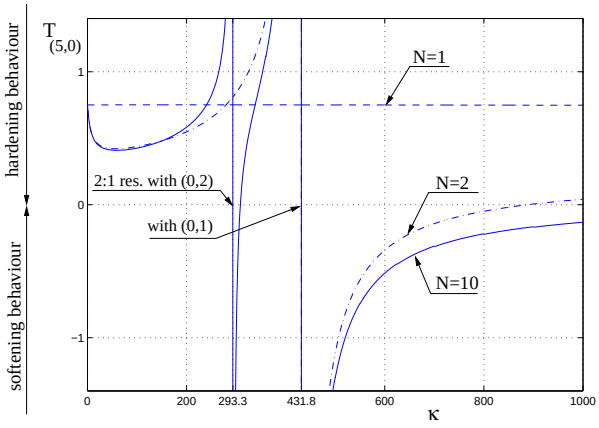

Figure 4. Type of non-linearity for mode (5,0) with respect to κ (solid line : converged result with N=10 modes). N=1: single-mode truncation (dashed line), N=2: two modes truncation ((5,0) and (0,1), dash-dotted line).

The result for the fundamental (2,0) mode is shown on Fig. 3. The hardening behaviour, typical of flat plates, is found for $\kappa = 0$. Then in favor of the 2:1 resonance with (0,1), the behaviour becomes softening at $\kappa = 2.68$, and returns to hardening at $\kappa = 4.98$. It must be noted that the values of $T_{(2,0)}$ after the 2:1 resonance are very small, so that one can conclude that the overall behaviour of this mode is neutral. It will be shown in the last section, concerned with experimental results, that the near-zero value of $T_{(2,0)}$ can change sign when taking into account some slight imperfections.

Modal convergence of the solution is also shown. The Dotted line shows the predicted type of non-linearity with a single-mode truncation. The converged result is shown with $N = 12$ modes, although a two-mode truncation (with (2,0) and (0,1)) gives excellent result. When increasing the number of nodal diameters k_p of the studied mode, the number of possible 2:1 resonances with other modes increases, as it can be seen on Fig. 2. Another typical example is shown on Fig. 4 for mode (5,0). Two 2:1 internal resonances are now possible: with mode (0,2) at $\kappa = 293.3$, and with (0,1) at $\kappa = 431.8$. The softening region caused by these resonances are very narrow and practically might be unobservable. Finally it is observed that the behaviour settles down to the softening case after the last 2:1 resonance. This feature is in fact general and has been observed for all the purely asymmetric modes, except the fundamental.

From these results and other which are not shown here for the sake of brevity, the following general conclusions can be drawn on the behaviour of purely asymmetric modes as a function of the geometry:

- The fundamental importance of axisymmetric modes on non-linear behaviour of asymmetric ones has been underlined. This feature is common to circular cylindrical shell vibrations [Amabili, Pellicano and Païdoussis, 1998].
- Hardening behaviour is observed until the 2:1 resonance with mode (0,1), where softening behaviour settles down, except fot the fundamental (2,0) mode, where neutral behaviour dominates.
- The type of non-linearity tends to zero as κ tends to infinity.
- The more nodal diameters the mode has, the more 2:1 internal resonances are possible. However, these resonances induce softening behaviour on a narrow region which is certainly unobservable.

4.2 Axisymmetric modes

The first two axisymmetric modes are here considered, namely mode (0,1) and (0,2). According to the rules defining modes that are able to act on the type of non-linearity, only the axisymmetric modes are considered, which substantially reduces the involved computations.

The main difference with previous section is the behaviour of the eigenfrequencies with respect to κ. As it can be seen on Fig. 2, axisymmetric eigenfrequencies increase with curvature. In particular, an infinity of 2:1 internal resonances are now possible, with all the other axisymmetric modes.

The result of computation is shown on Fig. 5 for mode (0,1). It can be seen that the effect of the geometry is much more pronounced than for the asymmetric modes: the inital hardening behaviour ($\kappa = 0$) becomes softening at $\kappa = 1.93$. Whereas the change of behaviour of purely asymmetric modes were only due to 2:1 resonance, here a geometrical effect acts first to change the behaviour for very small value of κ.

This is a consequence of the variations of the eigenfrequencies with curvature.

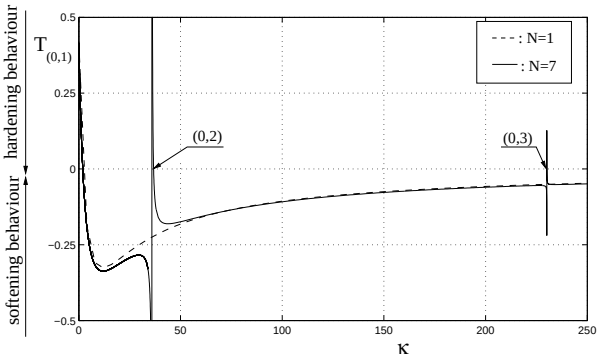

Figure 5. Type of non-linearity for mode (0,1) with respect to κ. Solid line : converged result with 7 modes. Dashed line: result given by the single-mode truncation.

Single-mode prediction is also shown on Fig. 5. Although the 2:1 resonances are missed, the general behaviour is correctly predicted: change from hardening to softening due to curvature is found at $\kappa = 1.95$ instead of $\kappa = 1.93$, and the asymptotic behaviour, which becomes neutral when κ tends to infinity, is recovered. These results show that for the specific case of the fundamental axisymmetric mode, the single-mode approximation predicts the essential features, in spite of a too severe truncation.

However, the importance of keeping numerous modes becomes evident for higher axisymmetric modes. Fig. 6 presents the convergence results for mode (0,2). Single-mode truncation predicts

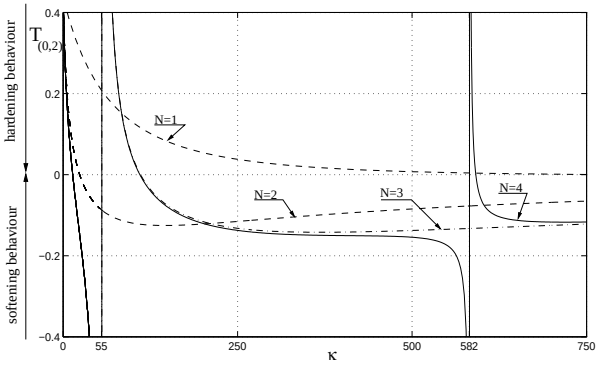

Figure 6. Effect of the number of modes retained in the summations for the type of non-linearity of mode (0,2). Dashed lines : N=1 (mode (0,2) only), and N=2: (0,1)+(0,2). Dash-dotted line (N=3): (0,1) to (0,3). Solid line (N=4): (0,1) to (0,4).

a hardening behaviour for every κ, which was the results found by [Yasuda and Kushida, 1984]. This prediction is corrected as soon as the (0,1) mode is kept for computation, but 2:1 resonances are missed. The result with $N = 4$ is acceptable since the essential features are predicted: transition to hardening to softening behaviour due to the geometric effect, at $\kappa = 13.73$; as well as the first two 2:1 resonances, respectively with mode (0,3) ($\kappa = 55.47$), and mode (0,4) ($\kappa = 582.3$).

From these results, some general rules can be deduced on the behaviour of axisymmetric modes:

- The effect of geometry is much more pronounced and leads to a softening behaviour which occurs rapidly, for small values of κ.
- 2:1 internal resonances with all other axisymmetric modes are possible. However, only the internal resonance with the next axisymmetric mode leads to a significant change of behaviour. The other implies a return to the hardening behaviour which occurs on a negligible interval.
- Except for the first (0,1) mode, where the single-mode approximation captures the essential features, numerous axisymmetric modes have to be kept in the computation.
- The type of non-linearity tends to zero as κ tends to infinity.

4.3 Mixed modes

The result for the first mixed mode, namely (1,1), is presented on Fig. 7. As for the axisymmetric modes, the effect of geometry is important and leads to a change of behaviour for a very small value of the aspect ratio: $\kappa = 5.3$. Then 2:1 internal resonances occurs, with modes (2,2), (0,3), (2,3), (0,4), ... Their number is unlimited, as for the axisymmetric case. The change of behaviour occurs on very small intervals, so that it has no chance to be experimentally observable. It can thus be concluded that except on a very small interval ($\kappa \in [0\,,\ 5.3]$), mode (1,1) behaves in a softening way.

The single-mode approximation is also shown on Fig. 7. It predicts a hardening behaviour which becomes neutral when κ tends to infinity. The converged result is obtained for $N = 17$ modes, namely : (1,1); (2,0) to (2,4); (0,1) to (0,5), and shows that, contrary to the precedent cases, coefficient $T_{(1,1)}$ tends to a finite value when κ tends to infinity. Hence the behaviour remains softening and does not becomes neutral for large values of the aspect ratio, which constitutes the main difference with the precedent case. Otherwise, the conclusions drawn are the same.

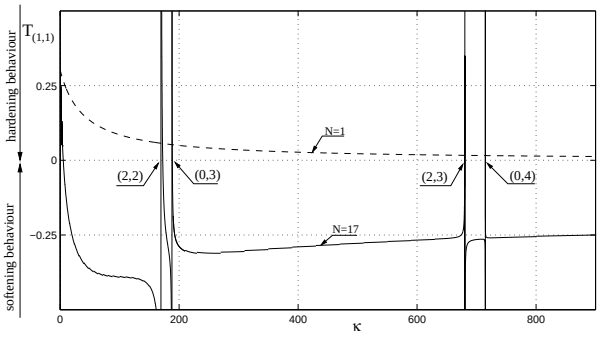

Figure 7. Type of non-linearity for mode (1,1). Single-mode approximation (N=1, dashed line) and converged result (N=17, solid line), are represented. The occurrence of 2:1 internal resonances with modes (2,2) (κ=169.4), (0,3) (κ=187.9), (2,3) (κ=680.4) and (0,4) (κ=714.7) are also shown.

5 Experimental measurements

5.1 Set-up

A series of measurements have been performed on two spherical shells, whose geometrical data are summarized in Table 1.

Shell	h	a	R	$R_{meas.}$	κ
	[mm]	[mm]	[mm]	[mm]	[adim]
1	1	300	4505	4158	399.1
2	1.5	300	1515	1480	1568.4

Table 1. Geometrical data of the two shells of the laboratory.

The aspect ratio of the first shell is very small, so that, at first sight, Shell No. 1 may not appear very different from a flat plate. As a consequence of the way they were built, the two shells are not perfect at all. In particular, their height, as a function of the radius r, has been precisely measured, showing that Shell No. 1 explicitely exhibits two different radius of curvature (see Fig. 8). Shell No. 2 has a more uniform and perfect radius of curvature.

When fitting the optimal radius of curvature for each shell, it has been found that R_1 was equal to 4158 mm (instead of 4505 mm), and R_2=1480 mm (instead of 1515 mm). These values are reported in Table 1, in the column $R_{meas.}$.

The consequences of this deviation to perfectness are twofold: first, the measured eigenfrequencies will strongly differ from the theoretical ones. This will be addressed in the next section. Secondly, the type of non-linearity will be difficult to fit to experimental measurements (see § 5.3).

The shell is excited at a choosen point by an electromagnetic device already used with success in other experiments led at the laboratory [Thomas, Touzé and Chaigne, 2003; Thomas, Luminais and Touzé, 2005]. The precise location of the excitation is adjusted for each measured mode, so as to coincide with an antinode. A scanning laser vibrometer is used to obtain the velocity of a single point as well as the spatial pattern of the studied mode, an essential information for a mode identification.

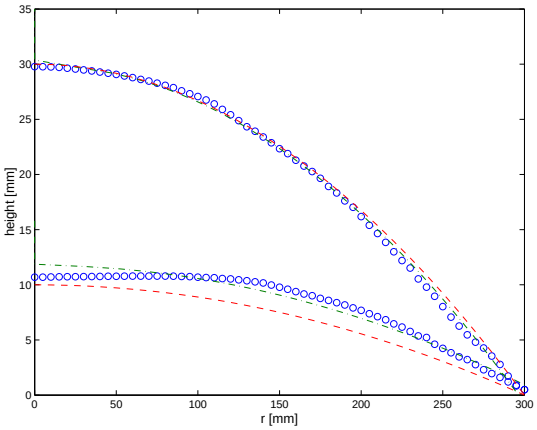

Figure 8. Measured profi le of the two tested shells. ○: experimental points, dashed line: radius of curvature provided by the manufacturer, dash-dotted: best fi t to experimental points.

5.2 Modal analysis

Modal analysis of the two shells has been performed. The results, expressed in adimensional frequencies, are reported in Table 2 for Shell No. 1, and in Table 3 for Shell No. 2. The relation from measured frequencies (in Hz) to adimensional ones has been estimated by linear regression on the first modes. For shell No. 1, great care has been brought to the measurement of the two preferential eigenfrequencies for asymmetric modes, to highlight the deviation from perfectness.

As it can be seen in Table 2, important discrepancies are present between axisymmetric measured and theoretical eigenfrequencies. This is the effect of the irregular curvature. A numerical study of doubly curved shallow spherical shells has shown that a change in curvature mainly influences the axisymmetric eigenfrequencies, as compared to the asymmetric ones, thus confirming the experimental evidence.

For shell No.2, the differences between theoretical and measured eigenfrequencies are less pronounced, although still present and significant for the first axisymmetric mode. This clearly shows that very slight imperfections and deviations from spherical perfectness have immediate and quantitative conse-

Shell No. 1			
Mode (k,n)	[theory]	[config. 1]	[config. 2]
(2,0)	5.45	9.48	9.86
(3,0)	12.80	15.88	16.24
(4,0)	22.43	23.40	24.13
(5,0)	34.21	31.69	34.52
(6,0)	48.09	43.71	48.28
(7,0)	64.06	59.30	61.49
(8,0)★	82.15	77.5	/
(0,1)	65.95	65.79	
(0,2)★	75.83	139.85	
(0,3)	109.44	224.20	

Table 2. Shell No.1. Comparisons between adimensional theoretical frequencies $\omega_{(k,n)}$ (second column) and measured frequencies (column 3 and 4 for preferential configurations if any). The ★ indicates that curve veering was present and thus the mode shape has not been clearly identified.

quences on the eigenfrequencies.

Shell No. 2		
Mode (k,n)	[theory]	[meas.]
(2,0)	5.52	7.08
(3,0)	13.12	15.05
(4,0)	23.21	25.02
(5,0)	35.53	36.56
(6,0)	49.94	49.15
(7,0)	66.36	61.84
(0,1)	130.29	84.38
(0,2)	135.56	126.3

Table 3. Comparisons between adimensional theoretical frequencies $\omega_{(k,n)}$ and measured frequencies for shell No. 2.

The second problem encountered during modal identification was due to curve veering. An example is shown in Fig. 9, where two experimental deflection shapes are shown. It can be seen that mode (8,0) presents a strong coupling with mode (1,1), resulting in a hybrid mode, which renders the identification difficult. All these experimental difficulties show that identification is very good for the first asymmetric modes, until the first axisymmetric. After the first axisymmetric mode, all the theoretical results are difficult to compare with measurement. Thus, the type of non-linearity will be mainly explored on the first asymmetric modes. This linear modal analysis clearly shows that imperfections are very important in the study of shallow spherical shells. This will be again discussed in the next subsection.

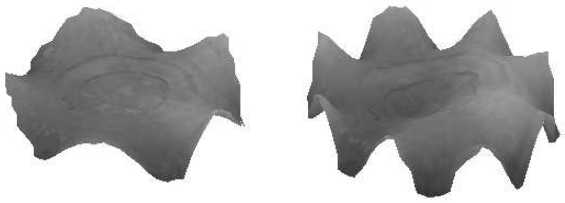

Figure 9. Measured mode shapes for modes (5,0) and (8,0).

5.3 Type of non-linearity

For the first modes of each shell, the backbone curve is measured by finding, for a number of fixed values of the excitation amplitude, the maximum of the resonance curve. The amplitude of excitation is first choosen at a very low level to ensure linear vibration and hence measurement of the linear eigenfrequency. Then the measurement is repeated by increasing the excitation amplitude, until mode coupling appears. Some modes show energy transfer and mode coupling for very low level of the excitation, thus making the measurement of the type of non-linearity impossible. This has been the case here for mode (4,0) of shell No.1, where the type of non-linearity is not reported.

Many differences occur between the perfect shell theoretically studied, and a real shell with slight imperfections. It has been seen during modal analysis that a very slight change of curvature may have a pronounced effect on the axisymmetric eigenfrequencies. Another effect of the imperfection is to split the single eigenfrequency of the two preferential configurations in two different eigenfrequencies which differs from a few Hertz. Fortunately, these two effects can be easily simulated by simply adjusting the eigenfrequencies in the model to their measured values. This has been realized so as to compute an "adjusted type of non-linearity", that takes into account the real eigenfrequencies (all the other quantities are kept). This trick allows one to compare three type of non-linearity: the measured one, the perfect one, and the adjusted one, where imperfections are taken into account into the eigenfrequencies only.

The obtained results for Shell No.1 are summarized in Table 4, and Fig. 10 illustrates four different cases. The first comment on Table 4 is that taking

into account the real eigenfrequencies of the shell can change the predicted type of non-linearity, see for example mode (2,0). The general behaviour of the type of non-linearity for the first asymmetric mode appears in fact to be soft for the first ones until, for a given κ, last 2:1 resonance with (0,1). Then hardening behaviour is predicted. This general feature is observed, but one can see that the transition from "soft modes" to "hard modes" is predicted to occur at mode (6,0) whereas it is measured at mode (7,0).

Shell No.1

Mode (k,n)	[perfect]	[adjusted]	[meas.]
$(2,0)_1$	+1.5e-3	-1.45e-3	-2e-3
$(2,0)_2$	+1.5e-3	-1.57e-3	-10e-3
$(3,0)_2$	-6e-3	-6.1e-3	-7e-3
$(5,0)_1$	+2.65	-2.73	-0.02
$(5,0)_2$	+2.65	+2.24	+.001
$(6,0)_1$	+0.62	+0.84	-0.08
$(6,0)_2$	+0.62	+0.59	-0.2
$(7,0)_2$	+0.56	+0.58	+0.14
(0,1)	-0.03	-0.03	-0.09

Table 4. Type of non-linearity for Shell No.1. First column: considered mode (the subscript refers to the preferential configuration). Second column: theoretical T_p, perfect case. Third column: adjusted theoretical T_p, obtained by changing the eigenfrequencies in the computation. Fourth column: best fit to experimental data

Results for shell No. 2 are reported in Table 5. As a consequence of the slighter imperfections of this shell, the results are much better. The transition from the first modes displaying softening behaviour to the others, is correctly predicted by the adjusted value of T_p, so that all the predictions have the good sign. The only difference is on the values of T_p, which differs (in the worst case) by a factor 9.

All these experimental results shows that imperfections are of major relevance in order to predict essential dynamical feature of a shallow spherical shell, such as the type of non-linearity which were here addressed. Shell No.1 exhibits strong discrepancies between prediction and measurement, even when the perfect eigenfrequencies are corrected to simulate the imperfections of the shell. Shell No.2 displays much better results, however, deviations are still observed. This indicates that fitting the eigenfrequencies to the measured ones is not enough to quantitatively predict the type of non-linearity. It shows, among other things, that imperfections have also a quantitative

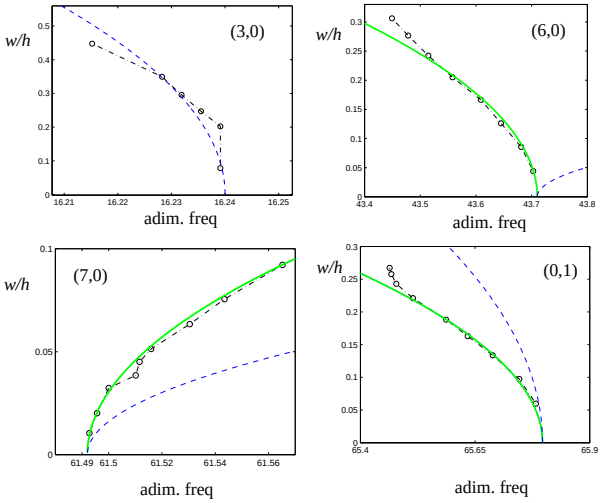

Figure 10. Backbone curves measured for shell No. 1 and for modes (3,0),config. 2; (6,0), config. 1; (7,0), config. 2, and (0,1). Dotted line: prediction given by the adjusted type of non-linearity, solid line: best fit to experimental data.

Shell No.2

Mode (k,n)	[perfect]	[adjusted]	[meas.]
(2,0)	+2e-4	-1.4e-4	-8.8e-4
(3,0)	-8.2e-5	-2.35e-3	-0.0017
(4,0)	-7.3e-3	-0.0207	-0.0133
(5,0)	-0.06	-0.2033	-0.0875
(6,0)	-0.305	+0.575	+0.062
(0,1)	-8e-3	-8.6e-3	-0.045

Table 5. Type of non-linearity for Shell No.2. First column: considered mode. Second column: theoretical T_p, perfect case. Third column: adjusted theoretical T_p,. Fourth column: best fit to experimental data

influence on the values of the physical coefficients $\{\beta_{ij}^p, \quad \Gamma_{ijk}^p\}$. This has also been observed in another experiment led in the laboratory, where a 1:1:2 internal resonance has been observed [Thomas, Luminais and Touzé, 2005]. The fitting of the quadratic terms led in this study reveals a factor 15 of difference between theoretical perfect quadratic coefficients and fitted ones.

6 Conclusion

The type of non-linearity for shallow spherical shells has been predicted by using NNMs. Important features have thus been put forward, *e.g.* the importance of axisymmetric modes in asymmetric vibrations in order to predict to correct type of non-linearity, or the role of 2:1 internal resonance in the transition from

the hardening (flat plate) behaviour to the softening one, obtained for large aspect ratio. Moreover, using NNMs to compute the correct trend of non-linearity avoids the shortcomings of single-mode truncation, without increasing the complexity of the calculations so as to renders them impracticable.

Experimental confrontations have revealed the importance of the imperfections, as very slight imperfections drastically change important features of the shell dynamics. For each of the two tested shells, deviation from perfectness has been clearly established with the non-uniform curvature observed. These imperfections have a huge effect on the eigenfrequencies of the shell, as well as on the dynamical features. The type of non-linearity can be easily adjusted by changing the eigenfrequencies to the measured ones in Eq. 8, so as to simulate the imperfections. By doing so, it has been observed that discrepancies are still observed between theoretical and measured T_p. This indicates that the imprefections also have a significant effect on the non-linear quadratic and cubic coefficients $\{\beta_{ij}^p\,,\ \ \Gamma_{ijk}^p\}$.

All these results shows that NNMs certainly provide the best method for easily computing the type of non-linearity. Slight imperfections have drastic and quantitative consequences, so that they also must be taken into account in order to reach convergence between theoretical developments and experimental measurements. Their effect must be taken into account in the way they change the eigenfrequencies, but also in the way they modify the non-linear coefficients.

Acknowledgments

The authors want to thank N. Georgescu-Roegen for committing the book [Georgescu-Roegen, 1971], as well as Pauline Béraud and Julien Capul for their help in the measurements of shell No. 2.

References

Amabili, M., Pellicano, F. and Païdoussis, M. P. (1998) Non-linear vibrations of simply supported, circular cylindrical shells, coupled to quiescent fluid. *J. Fluids Struct.*, **12**, pp. 883-918.

Amabili, M. and Païdoussis, M. P. (2003) Review of studies on geometrically non-linear vibrations and dynamics of circular cylindrical shells and panels, with and without fluid-structure interaction, *ASME J. Appl. Mech.*, **39**E, pp. 451-458.

Nayfeh, A.H., Nayfeh, J.F., and Mook, D.T. (1992) On methods for continuous systems with quadratic and cubic non-linearities, *Nonlinear Dynamics*, **3**, pp. 145-162.

Pellicano, F., Amabili, M., and Païdoussis, M. P. (2002) Effect of the geometry on the non-linear vibration of circular cylindrical shells, *Int. J. Nonlinear Mech.*, **37**, pp. 1181-1198.

Thomas, O., Touzé, C. and Chaigne, A. (2003) Asymmetric non-linear forced vibrations of free-edge circular plates. Part II: experiments, *J. Sound Vib.*, **265**, pp. 1075-1101.

Thomas, O., Touzé, C. and Chaigne, A. (2005) Non-linear vibrations of free-edge thin spherical shells: modal interaction rules and 1:1:2 internal resonance, *Int. J. Solids and Structures*, **42**(11-12), pp. 3339-3373.

Thomas, O., Luminais, E. and Touzé, C. (2005), Non-linear modal interactions in thin spherical shells: measurements of a 1:1:2 internal resonance, *Proc. third MIT Conference*, Boston, USA, June 14-17.

Touzé, C., Thomas, O. and Chaigne, A. (2004) Hardening/softening behaviour in non-linear oscillations of structural systems using non-linear normal modes, *J. Sound Vib.*, **273**, pp. 77-101.

Touzé, C., Thomas, O. and Huberdeau, A. (2004) Asymptotic non-linear normal modes for large-amplitude vibrations of continuous structures, *Computers and Structures*, **82**(31-32), pp. 2671-2682.

Yasuda, K. and Kushida, G. (1984) Nonlinear forced oscillations of a shallow spherical shell, *Bull. JSME*, **27**(232), pp. 2233-2240.

Georgescu-Roegen, N. (1971) The Entropy Law and the Economic Process, Harvard University Press, 1971.